



# Available online at www.sciencedirect.com

# **ScienceDirect**

Geochimica et Cosmochimica Acta 278 (2020) 244 260

# Geochimica et Cosmochimica

www.elsevier.com/locate/gca

# Silicate weathering in antarctic ice-rich permafrost: Insights using magnesium isotopes

Nicolas Cuozzo <sup>a,\*</sup>, Ronald S. Sletten <sup>a</sup>, Yan Hu <sup>a</sup>, Lu Liu <sup>a</sup>, Fang-Zhen Teng <sup>a</sup>, Birgit Hagedorn <sup>b</sup>

a Department of Earth and Space Sciences, University of Washington, Seattle, WA 98195, USA
b Sustainable Earth Research LLC, Anchorage, AK 99508, USA

Received 1 April 2019; accepted in revised form 15 July 2019; available online 24 July 2019

# Abstract

This study reports that substantial chemical weathering occurs at subzero temperatures in ice and salt rich permafrost in the McMurdo Dry Valleys, Antarctica. Chemical weathering is documented in a 30.0 m core collected in Beacon Valley by measuring the ionic composition, pH, and Mg isotopes of water extracted from thawed ice rich sediment. Evidence of rock weathering is revealed by coinciding increases in the Mg isotopic composition and pH values. The primary factor that controls weathering is the salt content that leads to unfrozen brine; this is most apparent in the upper 7.0 m where salt content is high, temperatures rise above 21 °C and modeled unfrozen water reaches up to 4.0% of ice content. In the upper 7.0 m, up to 60% of soluble Mg in the thawed permafrost ice is sourced from Ferrar Dolerite ( $\delta^{26}$ Mg = 0.22 ± 0.07‰) weathering, resulting in  $\delta^{26}$ Mg values ranging from of 0.82 ± 0.05‰ to 0.64 ± 0.05‰. Below 7.0 m, temperatures remain below 21 °C, unfrozen water is less than 2.0% of ice content, and on average, 5% of soluble Mg is sourced from dolerite weathering with  $\delta^{26}$ Mg values ranging from 1.05 ± 0.05‰ to 0.76 ± 0.05‰. Regions of the core that are modeled to have no unfrozen water show little or no evidence of chemical weathering and relatively constant  $\delta^{26}$ Mg values close to Taylor Glacier and Beacon Valley snowfall values (0.93 ± 0.06‰). This study demonstrates that significant chemical weathering occurs at subzero temperatures in permafrost where liquid brines form. © 2019 Elsevier Ltd. All rights reserved.

Keywords: Polar deserts; McMurdo Dry Valleys; Beacon Valley; Permafrost; Unfrozen water; Brine; Mars analog

# 1. INTRODUCTION

The McMurdo Dry Valleys (MDV) are among the cold est and driest regions on Earth and one of the few ice free regions in Antarctica. The environmental setting of the MDV is severe, with average summer and winter tempera tures below 0 °C, average precipitation less than 100 mm yr<sup>-1</sup> in the form of snowfall (Bromley, 1985; Doran et al., 2002; Fountain et al., 2010), no vascular plants (Alberdi et al., 2002), and landscapes dominated by

ice rich permafrost. Chemical weathering in permafrost environments such as the MDV is of interest because while permafrost is widespread, making up 24% of exposed land in the Northern hemisphere (Zhang et al., 1999) and around 25% of the Antarctic region (Bockheim, 1995; Schaefer et al., 2017), chemical weathering is not well documented in these environments, particularly in the Antarctic as it is less accessible and less studied compared to the northern hemisphere. Furthermore, they are considered one of the closest terrestrial analogs to the martian environment and can be used to better understand weathering processes occur ring in similar conditions on Mars (Anderson et al., 1972;

E mail address: ncuozzo@uw.edu (N. Cuozzo).

<sup>\*</sup> Corresponding author.

Gibson et al., 1983; Dickinson and Rosen, 2003; Wentworth et al., 2005; Heldmann et al., 2013).

Previous studies on chemical weathering in the MDV have found extensive salt accumulations, as is common in desert landscapes. Claridge and Campbell (1977) and Keys and Williams (1981) found major cations (Na<sup>+</sup>, Ca<sup>2+</sup>, Mg<sup>2+</sup>, and K<sup>+</sup>) accumulated over time from trans port and deposition of marine aerosols and chemical weath ering, with Mg concentrations particularly enriched in soils formed on dolerite parent material. Major anions (Cl<sup>-</sup>,  $SO_4^{3-}$ , and  $NO_3^{-}$ ) were found to be sourced from transport of marine aerosols and oxidation of reduced gaseous sulfur and nitrogen compounds (Bao et al., 2000; Michalski et al., 2005). Further studies have looked at solutes (Green et al., 1988; Lyons and Mayewski, 1993; Nezat et al., 2001) and isotopic composition, including Sr. Li, B, and Ca, (Jones and Faure, 1978; Witherow et al., 2010; Dowling et al., 2013; Leslie et al., 2014; Lyons et al., 2017) of lake waters, streams, and hyporheic zone sediments. These studies have suggested that silicate weathering must occur to explain the water composition in these regions. Physical evidence of rock and sediment alteration (<1 m) in the hyporheic zone are also documented in the MDV (Gibson et al., 1983; Dickinson and Grapes, 1997; Maurice et al., 2002; Wentworth et al., 2005; Tamppari et al., 2012; Marra et al., 2017; Heindel et al., 2018). While most of these stud ies focused on weathering in wetter regions at shallow depths in the MDV (streams, lakes, and hyporheic zones), only one study (Dickinson and Rosen, 2003) has looked at weathering processes in a deep permafrost profile using oxygen isotopes and ionic composition; however, they did not quantify the degree of weathering that occurs.

Magnesium isotopes have been used to study chemical weathering in soils (Pogge von Strandmann et al., 2008, 2012; Teng et al., 2010; Tipper et al., 2010, 2012a, 2012b; Huang et al., 2012; Opfergelt et al., 2012, 2014; Liu et al., 2014; Ma et al., 2015) and they can provide an estimate on the degree of weathering because of their fractionation properties (Galy et al., 2002; De Villiers et al., 2005; Liu et al., 2014). Large mass dependent fractionation of Mg isotopes can occur during low temperature chemical weath ering reactions, including dissolution, precipitation, and cation exchange (see review of Teng, 2017 and references therein). During chemical weathering, light Mg isotopes are preferentially released from silicate rocks to river waters, which end up in the ocean. This process results in a homogeneous and significantly lighter Mg isotopic com position of seawater ( $\delta^{26}$ Mg =  $0.83\%e \pm 0.09\%e$ , Ling et al., 2011), leaving variably heavier weathered residues in the upper continental crust ( $\delta^{26}Mg = 0.22\%$ , Li et al., 2010). The distinct isotopic values of these two reser voirs provide a tool to look at the mixing between Mg in the MDV derived from a seawater source (snowfall and gla cial ice), and a crustal silicate source (Ferrar Dolerite), and insight towards the degree of weathering.

The study presented here analyzes for Mg isotopes, pH, and ionic composition of water and sediment extracted from a thawed 30.0 m permafrost core collected in Beacon Valley. The chemical data are used to model the unfrozen water content and to quantify the contribution of Mg due

to dolerite weathering in the MDV permafrost. Our results reveal that significant silicate weathering occurs in subzero salt rich ice cemented permafrost environments and this finding provides new insights into weathering processes in ice cemented permafrost on Earth, as well as serving as an analog for weathering in martian permafrost.

#### 2. STUDY SITE

#### 2.1. Beacon Valley, Antarctica

The MDV are a hyperarid, polar desert that remain free of ice cover as a result of the high threshold of the Transantarctic Mountains, which divert ice from the East Antarctic Ice Sheet away from McMurdo Sound, and the Wilson Piedmont Glacier, which isolates the valleys from the Ross Sea and acts as a blockade to snow entering them (Chinn, 1990; Hall and Denton, 2002). Beacon Valley is one of the southern most Dry Valleys, trending northeast southwest and covering an area approximately 3 km wide and 12 km long (Fig. 1). Average annual temperatures are around 22.9 °C (Liu et al., 2015) with less than 100 mm/yr of precipitation in the form of snowfall (Fountain et al., 2010). The lower valley on its northeast end is bounded by Taylor Glacier, an East Antarctic Ice Sheet outlet glacier. Bedrock in Beacon Valley consists of Devonian to Jurassic Beacon Group sandstones, siltstones, and shales, with sills and dikes of tholeiitic Jurassic Ferrar Dolerite (McElroy and Rose, 1987).

The ice cemented permafrost core analyzed in this study was collected in the lower Beacon Valley (77°48′11.4″S, 160°42′49.8″E) as described below. The surface of Beacon Valley is covered by patterned ground with polygonal diameters of 10 20 m and the core was collected in the cen ter of a polygon, which is thought to be the most stable region (Linkletter et al., 1973; Sletten et al., 2003). Sediment in the Beacon Valley core is composed mostly of sand sized grains of quartz and dolerite that are cemented by an ice rich matrix. Sediment is massive and shows no evidence of stratification or facies changes. The sediment is believed to be sourced from glacial deposits and aeolian processes (Bockheim et al., 2009; Diaz et al., 2018), and based on modeled sublimation rates, the sediment age is estimated to be at least 1 Ma (Liu et al., 2015).

# 3. METHODS

# 3.1. Sample Collection

A 30.0 m ice cemented permafrost core was collected in lower Beacon Valley in 2008 and stored in a 30.0 °C free zer at the University of Washington, Seattle. Drilling began 0.4 m below the surface at the top of the ice cemented per mafrost. The upper 0.4 m consists of dry permafrost and was sampled separately. The permafrost core was cut into subsamples at 0.1 0.3 m intervals along its depth using a carbide tipped band saw. The frozen sediment samples were then thawed overnight in a refrigerator in sealed polyethy lene bags. The meltwater was extracted from the thawed sediments by centrifuging in a double bottom centrifuge

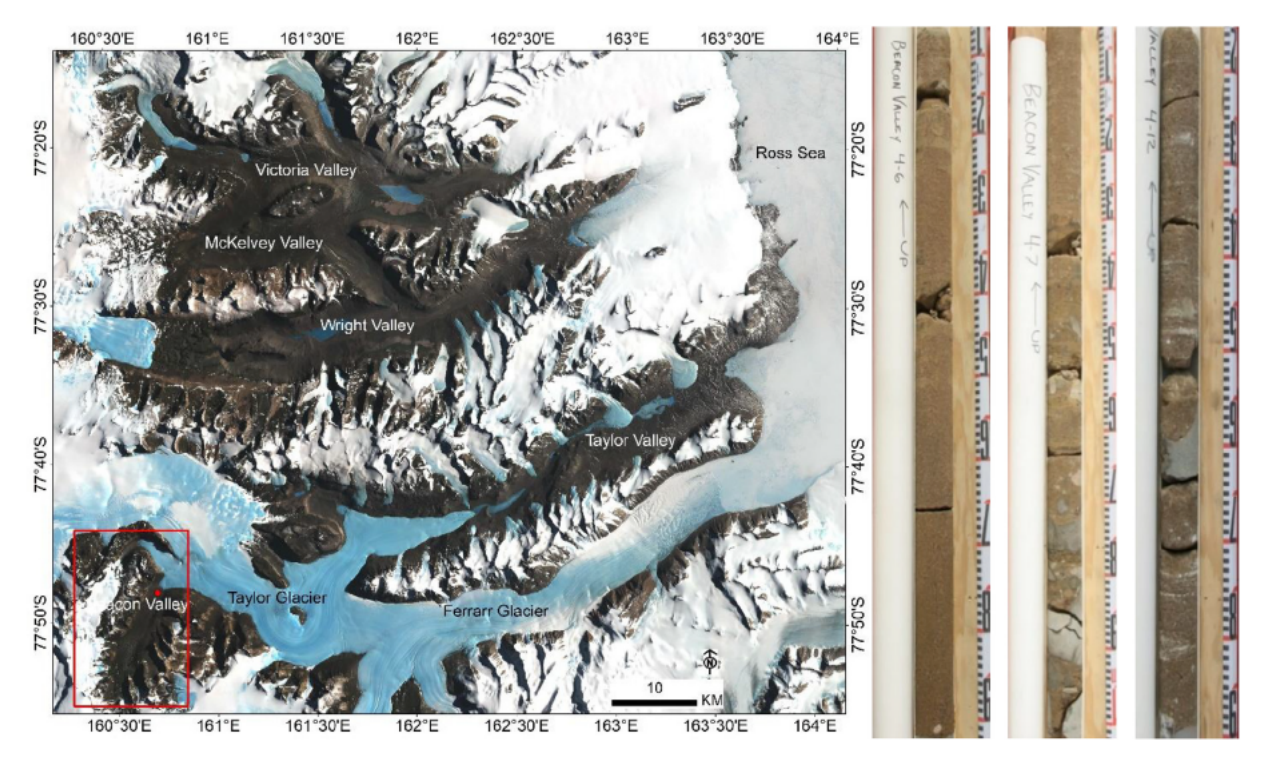


Fig. 1. (A) Landsat Image of Mosaic of the MDV (available at http://lima.usgs.gov/), with the location of the site (red dot) where the 30 m ice cemented permafrost core was collected; (B) Meter sections of the ice cemented permafrost core (6 m, 7 m, and 12 m from left to right).

cup (a perforated cup fitted with a 0.45 μm Nucleopore fil ter followed by a closed cup). The total ice content of each sample was determined gravimetrically. Large clasts of dolerite were collected from the Beacon Valley surface and sampled from the core at 0.6 and 2.2 m. Taylor Glacier Ice from an archived core (Nirvana) (Pettit et al., 2014) col lected near the terminus to Taylor Valley, as well as fresh Beacon Valley snowfall collected in the field were thawed and analyzed. Analyses were performed on three sets of samples: (1) water collected from thawed permafrost ice from the 30 m core, (2) permafrost sediment isolated from the 30 m core, and (3) thawed glacial ice and snow.

# 3.2. Compositional analysis

The soluble salts in the thawed permafrost ice, thawed glacial ice, and thawed snow samples were analyzed for major cations (Ca<sup>2+</sup>, Mg<sup>2+</sup>, Na<sup>+</sup>, K<sup>+</sup>) using Inductively Coupled Plasma Optical Emission Spectroscopy (ICP OES) (Perkin Elmer® Optima 3300 DV), major anions (Cl<sup>-</sup>, F<sup>-</sup>, SO<sub>4</sub><sup>2-</sup>, NO<sub>3</sub>) using Ion Chromatography (IC) (Dionex® ICS 2500), and pH using a WTW pH probe fitted with a SenTix 41 pH/temperature probe. The elemental composition of the <2 mm fraction of permafrost sediment and bulk rock samples was determined using a Thermo ARL X ray Fluorescence Spectrometer (XRF) at the GeoAnalytical Lab at Washington State University. The weathered rind of the bulk rock samples was removed and only the unweathered rock was used for analysis. The <2 mm fractions of permafrost sediment were powdered and analyzed for their mineralogy using Rigaku MiniFlex

600 benchtop X ray diffractometer (XRD) with a D/teX high speed detector and Co Kα radiation. Data were col lected at a step size of 0.02° per minute step counting rate, from 2 to 80° 20 at 15 mA and 40 kV in the X ray Diffrac tion Laboratory located at NASA Johnson Space Center. Samples were prepared in aluminum holders, and the XRD instrument was operated under ambient conditions and calibrated with the National Institute of Standards and Technology (NIST) silicon standard, and a NIST lan thanum hexaboride standard is used to characterize the instruments line broadening function. Rietveld refinement was carried out using MDI Jade Software with initial struc ture parameters for crystalline phases from the RRUFF database. Background patterns were fit by a polynomial and peaks were modeled by a pseudo Voigt profile func tion. Pattern overlays of standard phyllosilicates (Clay Mineral Repository) with known RIR and FWHM were used in Rietveld Refinements to estimate abundances of phyllosilicates in bulk samples.

# 3.3. Temperature measurements

A long term record of hourly temperatures is being recorded in a polygon adjacent to the one that was cored in Beacon Valley at depths of 1.25, 2.5, 5.0, 10.0, 20.0, and 30.0 m. The temperatures are measured using a Camp bell CR10X 2M data logger with Campbell 107 thermistor temperatures probes. The yearly maximum and minimum temperature for each depth is then interpolated to create a maximum and minimum temperature at each sampling depth.

# 3.4. Geochemical modeling

The equilibrium thermodynamic models, PHREEQC (Version 3 using ColdChem database) and FREZCHEM (Version 13.2), were used to model the unfrozen water con tent and secondary salt precipitation at each sample depth of the core based on the chemical composition of the thawed permafrost ice and using the interpolated maximum temperature. As the water freezes, ions are excluded from the ice phase and concentrate in the water, thereby depressing the freezing point of the brine (Low et al., 1968; Tice et al., 1985). PHREEQC and FREZCHEM use Pitzer equations to model these high ionic strength solutions and are capable of modeling freezing of concentrated solutions down to 70 °C (Marion and Grant, 1994).

# 3.5. Particle Size Analysis

Particle size analysis was performed on  $\sim 1$  g permafrost sediment samples. Samples were split using a sample split ter to avoid sampling bias and analyzed using a laser diffraction particle size analyzer (Beckman Coulter LS 13 320). Samples were dispersed using an ultrasonic probe with the addition of 5 mL of 0.05% sodium bicarbonate sodium hexametaphosphate to keep the samples in suspen sion. Each sample was analyzed three times for reproducibility.

#### 3.6. Magnesium Isotope Analysis

Magnesium isotopes were analyzed in water samples from the thawed permafrost ice of the core. Beacon Valley snowfall, and Taylor Glacier ice. In addition, dolerite sam ples collected from the core and the surface of Beacon Val ley were analyzed. Rock digestion, chemical separation, and isotopic analysis were performed at the Isotope Labo ratory at the University of Washington, following the meth ods detailed in Teng et al. (2007) and Yang et al. (2009). The rocks were sampled to avoid any weathering rinds, crushed into a powder, and dissolved sequentially using Optima grade concentrated HF HNO3, HNO3 HCl, and HNO<sub>3</sub>. The water samples were evaporated to contain 5 40 μg Mg. Separation of Mg was achieved by loading 100 µL of sample dissolved in 1 N HNO<sub>3</sub> on a cation exchange chromatography column containing pre cleaned Bio Rad AG50W X8 resin (200 400 mesh) and was eluted using sequential additions of 1 N HNO<sub>3</sub>. This procedure is repeated twice for each sample to ensure purification.

Magnesium isotopic ratios were measured on a Nu Plasma II Multi Collector ICP MS using standard sample bracketing (alternating measurements of samples and stan dards) for correction of instrumental fractionation (Teng and Yang, 2014). Magnesium isotopic data are reported in delta ( $\delta$ ) notation, which represents parts per thousand (‰) deviations of the ratio between the sample and stan dard, where X refers to mass 25 or 26:

$$\delta^{x}Mg(\%co) = 1000 \times \left\{ \left( \frac{(Mg/^{24}Mg)_{simple}}{(Mg/^{24}Mg)_{DSM3}} - 1 \right) \right\} \left( \frac{(Mg/^{24}Mg)_{DSM3}}{(Mg/^{24}Mg)_{DSM3}} - 1 \right)$$

The accuracy of the analysis was assessed using two in house standards (Hawaiian Seawater and San Carlos Oli vine) and two USGS rock standards (BHVO Basalt and MAG 1 Marine Mud). The results of these standards (Table 1) agree with recommended values (Teng et al., 2015; Hu et al., 2016).

#### 4. RESULTS

Physical and chemical parameters that were measured along the core's depth are reported below, including soluble salts, temperature, ice content, modeled unfrozen water content, pH, particle size, elemental composition of bulk sediment, and Mg isotopic composition:

#### 4.1. Ionic composition and pH of thawed permafrost ice

The thawed permafrost ice contains high concentrations of total soluble salts with an average value of 29 mmol/kg and a standard deviation (1SD) of 11.9 in the upper 7.0 m of the core and lower concentrations below 7.0 m with an average value of 19 mmol/kg (1SD = 8.1) (Fig. 2a and b). Two sample t tests comparing the mean total concentra tions revealed the concentrations in the two sections of the core were significantly different (p < 0.05). Na is the most concentrated cation, followed by Ca, Mg, and K. pH values were measured starting at the ice table at 0.4 m (Fig. 2c). The top four samples have pH values of 6.60 and rapidly increase toward the highest measured pH of 7.70. Excluding those four samples, pH values in the upper 7.0 m are consistently higher than the lower section of the core, with a mean value of 7.29 (1SD = 0.15). At  $7.0 \,\mathrm{m}$ , pH values drop down to a pH of 7.00 and remain around 7.00 until 18.0 m. From 18.0 to 30.0 m, the pH values increase from pH of 7.00 to 7.57. Two sample t tests also show a significant difference between the pH values of the upper and lower sections of the core (p < 0.05).

# 4.2. Temperature

Interpolated maximum and minimum monthly averaged borehole temperatures in Beacon Valley remain below 0 °C throughout the year with seasonal variation most prominent in the upper layers of the permafrost (Fig. 2d). The sediment closest to the surface has the most extreme tem perature highs and lows, ranging from 10 °C in the sum mer to 35 °C in the winter. Moving further down the core, these seasonal variations become less pronounced, and at 20.0 m, there is virtually no seasonal variation with temper ature steady at approximately 23 °C.

# 4.3. Ice content

The core can be grouped into three sections based on its ice content (Fig. 2e): 0.4~7.0~m, 7.0~18.0~m, and 18.0~30.0~m. From 0.4~to~7.0~m, the average ice content is 26.0~wt.% (1SD = 0.19). There are three outliers in the upper 7.0~m with ice content near 80~wt.% which reflect sev eral small ice lenses in the sediment. Excluding these three values, the average ice content reduces from 26.0~to

Table 1
Magnesium isotopic composition of standards run between the samples.

Standard	n	$\delta^{26}$ Mg	2SD	$\delta^{25}$ Mg	2SD
Hawaii Seawater (in house)		0.88	0.05	0.45	0.05
		0.89	0.05	0.46	0.04
		0.88	0.05	0.46	0.04
		0.86	0.05	0.44	0.06
		0.92	0.06	0.51	0.05
		0.85	0.06	0.48	0.05
		0.83	0.05	0.41	0.06
Average	7	0.87	0.05	0.46	0.05
Ling et al. (2011)	90	0.83	0.09	0.43	0.06
San Carlos Olivine		0.24	0.05	0.15	0.05
		0.20	0.05	0.13	0.05
		0.22	0.05	0.12	0.04
		0.25	0.05	0.11	0.06
		0.23	0.05	0.13	0.06
		0.25	0.03	0.16	0.04
		0.30	0.06	0.16	0.07
Average	7	0.24	0.05	0.14	0.05
Hu et al. (2016)	28	0.24	0.03	0.12	0.02
BHVO (USGS)		0.24	0.06	0.11	0.05
Basalt, Hawaii Volcanic Observatory		0.27	0.06	0.14	0.05
Average	2	0.26	0.06	0.13	0.05
Teng et al. (2015)		0.21	0.04	0.12	0.03
MAG 1 (USGS)		0.35	0.06	0.16	0.05
Marine Mud, Gulf of Maine		0.30	0.06	0.14	0.05
Average	2	0.32	0.06	0.15	0.05
Teng et al. (2015)		0.25	0.05	0.11	0.04

Results of Mg standards (n = number of analyses) run between the samples. Bolded values represent the average value of the standards in each run and italicized values represent the literature values. 2SD of Mg isotopic values represents two standard deviations of the bracketing standard measurements during a full analytical session.

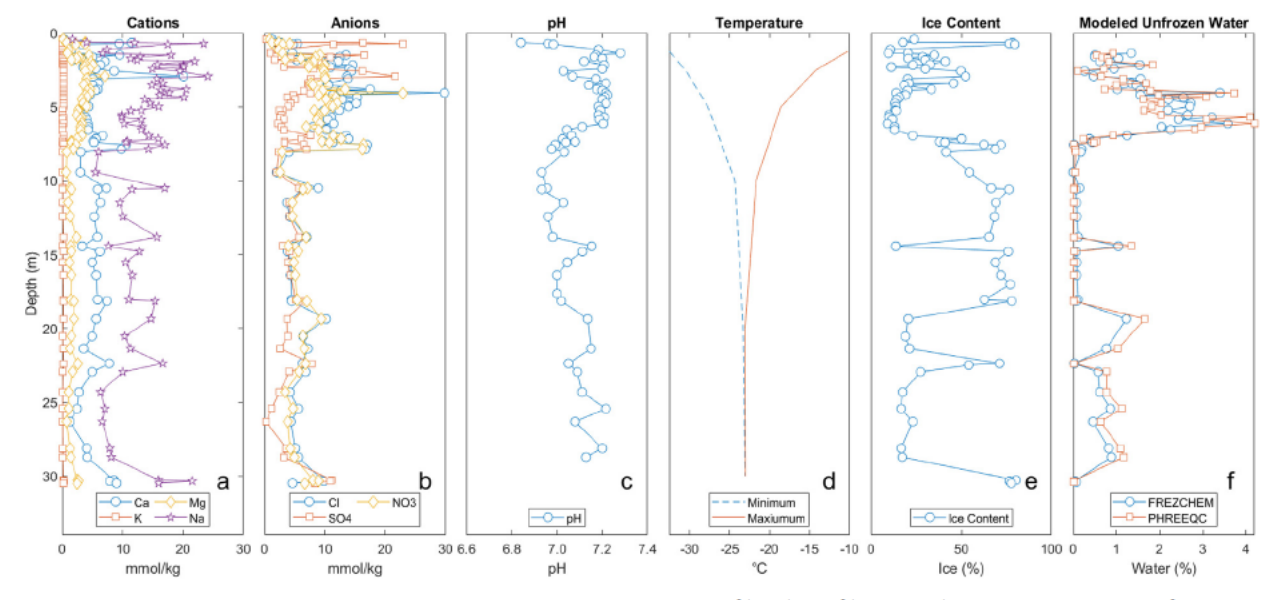


Fig. 2. Analytical result along the depth of the 30 m permafrost core for: (a) Ca<sup>2+</sup>, K<sup>+</sup>, Mg<sup>2+</sup>, and Na<sup>+</sup> (mmol/kg); (b) Cl , SO<sub>4</sub><sup>2</sup> , and NO<sub>3</sub> (mmol/kg); (c) pH; (d) Annual maximum and minimum temperatures (°C); (e) Ice content (%) measured gravimetrically; and (f) Modeled unfrozen water content (%) using FREZCHEM and PHREEQC. Most analyses show a major shift at 7 m depth, with cations, anions, pH, and modeled unfrozen water content higher in the upper 7 m section, and lower in the 7 30 m section. Temperatures have large seasonal variation in the upper 10 m of the core, and little seasonal variation below 10 m.

21.7 wt.% (1SD = 0.12). At 7.0 m, there is an abrupt increase in the ice content to approximately 50 wt.%. Excluding one outlier at 14.0 m, where the ice content is 13.6 wt.%, the average ice content from 7.0 to 18.0 m is 62.7 wt.% (1SD = 0.13). From 18.0 to 30.0 m, ice content decreases to an average ice content of 23.3 wt.% (1SD = 0.11), excluding two ice lenses at 22.0 m and  $30.0 \, \text{m}$ 

#### 4.4. Modeled unfrozen water content

Based on the soluble ions in the thawed permafrost and the temperature, equilibrium geochemical modeling using PHREEQC (Version 3, ColdChem database) and FREZ CHEM (Version 13.2) reveal substantial unfrozen water is present in the permafrost core at various depths (Fig. 2f). In the upper 7.0 m of the core, the unfrozen water content generally increases with depth and reaches a maximum of 4.0% of the ice content near 7.0 m. This section of the core experiences higher summer temperatures and higher con centrations of soluble salts that depress the freezing point of water. From 7.0 to 18.0 m, most samples have less than 0.1% unfrozen water content. Average temperatures are lower and there is a lower concentration of soluble salts to depress the freezing point. From 18.0 to 30.0 m, unfrozen water content increases up to 1.7% Despite the lower aver age temperature, this section has higher soluble salt concen trations than 7.0 18.0 m. These models do not consider particle size, pore space size, or ice lens formation, which may have a small effect on the amount of unfrozen water (Anderson and Morgenstern, 1973).

# 4.5. Particle size

Particle size of permafrost sediment was analyzed for the < 2 mm fraction (Fig. 3). Both the clay and silt sized fraction (<2 50 µm) and the sand sized fraction (50 2000  $\mu$ m) display a significant difference (p < 0.05)

between the upper 7.0 m and the lower 7.0 30.0 m. The clay and silt sized content in the upper 7.0 m increases with depth and has an average value of 6.4% with a standard deviation of 3.3. The clay and silt sized content in the lower 7.0 30.0 m has a more consistent distribution with a higher average value of 9.0% and a standard deviation of 1.9. Most of the permafrost sediment in the <2 mm fraction consists of sand sized particles (50 2000 µm). In the upper 7.0 m, sand on average makes up 93.6% (1SD = 3.3) of the sediment, and in the lower 7.0 30.0 m, sand on average makes up 91% (1SD = 1.9) of the sediment.

#### 4.6. Major element composition and minerology

XRF analysis of the <2 mm fraction of permafrost sed iment and unweathered Beacon Sandstone and Ferrar Dolerite is presented in Table 2 as oxides in weight percent (wt.%) normalized to 100%. Beacon Sandstone is composed almost entirely of SiO2 (>99 wt.%), with little to no MgO (<0.01 wt.%), while Ferrar Dolerite is composed primarily of SiO<sub>2</sub> (57 wt.%), Al<sub>2</sub>O<sub>3</sub> (14 wt.%), FeO\* (10 wt.%), CaO (9 wt.%), and MgO (5 wt.%). Major element composition of the permafrost sediment suggests a mixed lithology of sandstone and dolerite. XRD analysis of the permafrost sediment also suggests most of the sediment is composed of quartz, pyroxene (augite and orthopyroxene), and feld spar (andesine, anorthite, and orthoclase), with smaller amounts of gypsum (2 samples with <1%), muscovite, kaolinite, and saponite (Table 3).

On average, the permafrost sediment is composed mainly of  $SiO_2$  (80 wt.%, 1SD = 1.9). While the  $SiO_2$  con centration varies by only a few percent, there is a statisti cally significant difference between the upper 7.0 m and the lower 7.0 30.0 m (p < 0.05). CaO and MgO concentra tions are also statistically different (p < 0.05) in the upper and lower sections of the core, showing a decrease in the upper 7.0 m and remaining constant in the lower 7.0 30.0 m. K<sub>2</sub>O, Na<sub>2</sub>O, and Al<sub>2</sub>O<sub>3</sub> remain constant through

95

100

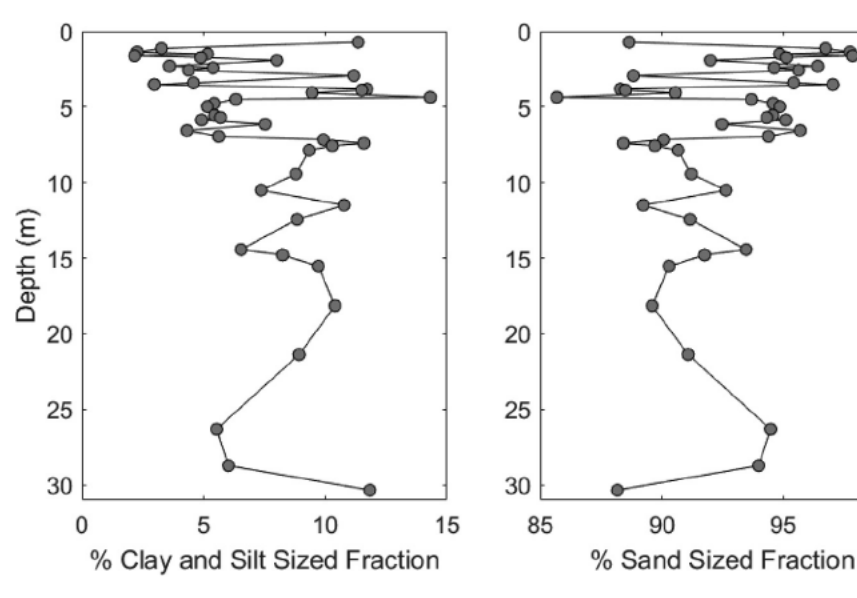


Fig. 3. Clay and silt sized and sand sized fractions of Beacon Valley core sediment. The upper 7.0 m have larger variation between samples while the lower 7.0 30.0 m have smaller variation in the texture. Sand sized particles make up at least 85% of sediment in each sample.

Table 2
Elemental abundance of Beacon Core Sediment samples determined by X ray fluorescence.

Sample Type	Sample ID	Depth (m)	XRF	LOI Normalized Major Elements (wt%)								
			SiO <sub>2</sub>	TiO <sub>2</sub>	$Al_2O_3$	FeO*	MnO	MgO	CaO	Na <sub>2</sub> O	K <sub>2</sub> O	$P_2O_5$
Permafrost Sediment	BV4 24 27	0.66	78.69	0.60	6.90	5.38	0.10	2.24	4.16	0.89	0.95	0.08
	BV4 105 113	1.49	75.34	0.86	7.75	6.47	0.12	2.50	4.69	1.03	1.15	0.08
	BV4 189 192	2.31	77.26	0.78	7.21	5.88	0.11	2.23	4.32	1.02	1.11	0.08
	BV4 269 271	3.10	81.82	0.46	6.04	4.28	0.08	1.94	3.63	0.79	0.89	0.06
	BV4 340 343	3.82	81.15	0.46	6.68	4.39	0.08	1.76	3.44	0.88	1.08	0.07
	BV4 395 397	4.36	78.61	0.53	7.54	5.03	0.09	2.01	3.96	1.00	1.15	0.08
	BV4 455 460	4.98	79.58	0.49	7.30	4.73	0.09	1.84	3.72	1.00	1.17	0.08
	BV4 529 532	5.71	79.34	0.52	7.28	4.86	0.09	1.89	3.77	1.00	1.17	0.08
	BV4 613 618	6.56	79.30	0.51	7.45	4.77	0.09	1.83	3.70	1.04	1.24	0.08
	BV4 653 656	6.95	79.46	0.51	7.36	4.75	0.09	1.79	3.72	1.04	1.20	0.08
	BV4 675 677	7.16	81.52	0.47	6.60	4.26	0.08	1.71	3.34	0.86	1.07	0.07
	BV4 744 748	7.86	81.96	0.43	6.59	4.08	0.08	1.64	3.24	0.83	1.08	0.07
	BV4 763 768	8.06	80.51	0.49	7.06	4.49	0.08	1.72	3.49	0.93	1.14	0.07
	BV4 1005 1016 (A & B)	10.51	80.68	0.48	6.93	4.47	0.08	1.77	3.49	0.90	1.13	0.07
	BV4 1108 1110	11.49	81.04	0.46	6.99	4.26	0.08	1.71	3.38	0.85	1.16	0.07
	BV4 1202 1204 (A & B)	12.43	81.35	0.47	6.80	4.26	0.08	1.66	3.36	0.84	1.11	0.07
	BV4 1438 1440 (A & B)	14.79	81.57	0.45	6.63	4.23	0.08	1.71	3.32	0.85	1.10	0.07
	BV4 2096 2098	21.37	80.81	0.43	7.01	4.26	0.08	1.81	3.58	0.93	1.02	0.06
	BV4 2830 2833	28.72	81.93	0.41	6.44	4.11	0.08	1.74	3.44	0.82	0.97	0.06
	BV4 3007 3010	30.49	76.55	0.60	8.43	5.44	0.10	2.11	4.31	1.10	1.28	0.08
Bulk Rock	Dolerite 2	0.60	57.65	0.97	13.89	10.66	0.18	4.20	8.73	2.14	1.43	0.15
	Dolerite 3	2.20	56.80	0.90	14.35	10.01	0.18	5.11	9.29	2.03	1.22	0.13
	Beacon Sandstone 1	surface	99.81	0.02	0.15	0.02	0.00	0.02	0.03	0.00	0.03	0.01
	Beacon Sandstone 2	surface	99.53	0.11	0.35	0.03	0.00	0.01	0.00	0.00	0.06	0.01
	Vida Granite	surface	69.41	0.34	15.44	2.93	0.06	0.39	1.89	3.68	5.78	0.07

Values are normalized to loss on ignition (LOI) weight. FeO\* is total Fe represented as FeO.

Sample ID	XRD Analysis											
	Quartz	Andesine	Augite	OPX	Anorthite	Orthoclase	Gypsum	Muscovite	Kaolinite	Saponite		
BV4 105 113	51.2	13.5	9.6	8.7	4.0	3.6	0.9	0.8	0.7	5.3		
BV4 269 271	62.4	13.8	7.7	6.3	4.2	4.2	0.0	1.4	0.6	3.4		
BV4 529 532	61.2	12.7	8.6	4.5	0.0	6.4	0.0	1.9	1.1	2.9		
BV4 763 768	61.5	15.2	5.8	8.8	0.0	0.0	0.5	1.0	1.7	4.6		
BV4 2096 2098	59.8	14.2	6.5	4.9	0.0	6.7	0.0	1.1	0.9	4.1		
BV4 2830 2833	62.1	13.4	5.2	6.9	0.0	4.6	0.0	2.0	0.7	4.9		

Table 3
Mineralogy (% abundance) of Beacon Valley core sediment determined by X ray diffraction.

out the 30.0 m core and show no statistical difference in the upper and lower sections.

# 4.7. Magnesium isotopes

Magnesium isotopic ratios of the thawed permafrost ice, bulk rock samples, thawed Taylor Glacier ice, and Beacon Valley snowfall are reported in Table 4. There are two Mg reservoirs in Beacon Valley with distinct Mg isotopic com positions. Dolerite samples collected from the core and the surface of Beacon Valley have an average Mg isotopic com position of  $0.22 \pm 0.07\%$  (n = 3), which is typical for basaltic rocks (Teng. 2017). Taylor Glacier/Beacon Snow fall samples have a significantly lower average Mg isotopic composition of  $0.93 \pm 0.06\%$  (n = 4), which is close to the seawater Mg isotopic composition of  $0.83 \pm 0.09\%$ (Ling et al., 2011). In the upper 7.0 m, the Mg isotopic com position of the thawed permafrost ice samples falls between these two end members, and in the lower 7.0 30.0 m, Mg isotopic composition falls within the Taylor Glacier/Beacon Snowfall range (Fig. 4).

The Mg isotopic composition in the upper 7.0 m can be further distinguished at 0.4 1.5 m and 1.5 7.0 m. At 0.4 m, the Mg isotopic composition is the highest recorded in the thawed permafrost ice with a  $\delta^{26}$ Mg value of  $\pm 0.05\%$  and lies directly at the boundary between the dry permafrost and ice cemented permafrost. Moving down towards 1.5 m, the Mg isotopic composition decreases to a  $\delta^{26}$ Mg value of 0.81  $\pm$  0.05‰. These upper samples, which are almost all heavier than the Taylor Glacier/Beacon Snow fall end member, are sampled from the section containing multiple ice lenses. From 1.5 to 7.0 m, Mg isotopic ratios start with a value of  $0.82 \pm 0.05\%$ , close to that of Taylor Glacier/Beacon Snowfall ( $0.93 \pm 0.06\%$ ), and gradually increase to  $0.64 \pm 0.05\%$  near 7.0 m. From 7.0 to 30.0 m,  $\delta^{26}$ Mg values are consistently lighter than above 7.0 m, aver aging 0.93%. These values in the lower section of the core are mostly within the range of the Taylor Glacier/Beacon Snowfall end member isotopic composition but show a slight increasing trend in Mg isotope composition with depth. In addition, two samples are significantly lighter than the Tay lor Glacier/Beacon Snowfall end member.

# 5. DISCUSSION

In this section, we present evidence of chemical weather ing in permafrost sediment and ice, discuss the controls over chemical weathering, and quantify the extent of weath ering using Mg isotopic composition. We discovered that Antarctic permafrost provides a unique environment where leaching is very limited and products from chemical weath ering reactions tend to remain in the permafrost over time, providing a record of these reactions. As discussed below, this accumulation of weathering products coincides with changes in ionic content, pH values, and Mg isotopes of the thawed permafrost ice over the sampling depth.

# 5.1. Magnesium in the MDV

Magnesium in Beacon Valley permafrost is primarily sourced from two reservoirs: (1) marine aerosols, and (2) chemical weathering of Ferrar dolerite (Claridge and Campbell, 1977; Keys and Williams, 1981). The first source of Mg, marine aerosols, is deposited by dust, katabatic winds, and snowmelt events which may sublimate or melt during strong solar radiation in summer months thereby releasing any entrained salts (Liu et al., 2015). Due to the hyperarid conditions of the MDV, ions released by snowfall become enriched over time and sediment eventually becomes brine rich with a depressed freezing point (Anderson and Morgenstern, 1973; Murrmann, 1973; Hagedorn et al., 2010). These brine films, along with salts inherited during sediment deposition, persist thorughout the depth of the permafrost.

Ferrar dolerite is the second major source of Mg in Bea con Valley and dolerite rock fragments are found throughout Beacon Valley. Ferrar dolerite is a medium to fine grained mafic igneous rock with a bulk composition consisting mainly of calcium rich plagioclase (An<sub>89</sub>Ab<sub>11</sub>) and magnesium rich pyroxene (Wo<sub>4</sub>En<sub>81</sub>Fs<sub>15</sub>), with accessory biotite, hornblende and iron oxides (Gunn, 1962; Campbell and Claridge, 1987; Elliot et al., 1995;). Three key reactions dictate the weathering products of Ferrar Dolerite:

$$(Ca_{0.4}, Mg_{0.8}, Fe_{0.15})SiO_{3(s)}(enstatite) + H_2O + 2H^+$$

$$\rightarrow (\mathcal{A}a_{0.4}^{2+}, Mg_{0.8}^{2+}, Fe_{0.15}^{2+})_{(aq)} + H_4SiO_{4(aq)}$$

$$CaAl_2Si_2O_{8(s)}(anorthite) + H_2O + 2H^+$$

$$\rightarrow Ca^{2+}_{(aq)} + Al_2Si_2O_5(OH)_4$$

$$2NaAlSi_3O_{8(s)}(albite) + 9H_2O + 2H^+$$

$$\rightarrow 2Na^{2+}_{(aq)} + Al_2Si_2O_5(OH)_4 + 4H_4SiO_{4(aq)}$$

These weathering reactants and products will be used to trace the extent of chemical weathering that occurs in the permafrost.

Table 4
Magnesium isotopic composition of Beacon Valley thawed permafrost ice, bulk rock, and Taylor Glacier/Beacon Snow samples. Depth from the surface is given as midpoint of sample collected.

Sample Type	Sample Name	Midpoint Depth (m)	$\delta^{26} Mg$	2SD	$\delta^{25} Mg$	2SD
Thawed Ice	BV4 0 4.5 (BV001)	0.42	0.52	0.05	0.23	0.05
	BV4 22 24	0.63	0.70	0.05	0.34	0.05
	BV4 28 35	0.72	0.70	0.05	0.39	0.05
	BV4 34.5 39.5 (BV002)	0.77	0.74	0.05	0.38	0.05
	BV4 93 100	1.37	0.80	0.05	0.42	0.05
	BV4 105 113	1.49	0.81	0.05	0.44	0.05
	BV4 120 123	1.62	0.82	0.05	0.42	0.05
	BV4 130 135	1.73	0.82	0.05	0.44	0.05
	BV4 142 143	1.83	0.77	0.05	0.41	0.05
	BV4 150 154	1.92	0.79	0.05	0.42	0.05
	BV4 189 192	2.31	0.75	0.05	0.40	0.05
	BV4 200 203	2.42	0.68	0.05	0.34	0.05
	BV4 215 219	2.57	0.73	0.05	0.37	0.05
	BV4 269 271	3.10	0.71	0.05	0.39	0.05
	BV4 340 343	3.82	0.68	0.05	0.38	0.05
	BV4 347 350	3.89	0.67	0.05	0.35	0.05
	BV4 364 368	4.06	0.63	0.05	0.33	0.05
	BV4 379 382	4.21	0.65	0.05	0.34	0.05
	BV4 395 397	4.36	0.68	0.05	0.36	0.04
	BV4 455 460	4.98	0.68	0.05	0.37	0.04
	BV4 483 488 (BV005)	5.26	0.64	0.05	0.34	0.04
	BV4 529 532	5.71	0.63	0.05	0.32	0.04
	BV4 573 575	6.14	0.68	0.05	0.35	0.04
	BV4 613 618	6.56	0.65	0.05	0.35	0.04
	BV4 653 656	6.95	0.64	0.05	0.34	0.04
	BV4 675 677	7.16	0.76	0.05	0.41	0.04
	BV4 698 702	7.40	0.89	0.05	0.45	0.04
	BV4 744 748	7.86	0.95	0.05	0.49	0.04
	BV4 902 905	9.44	1.02	0.03	0.54	0.04
	BV4 1005 1016a	10.51	0.92	0.05	0.49	0.04
	BV4 1108 1110	11.49	0.97	0.05	0.52	0.06
	BV4 1202 1204 (A & B)	12.43	0.98	0.05	0.50	0.06
	BV4 1438 1440 (A & B)	14.79	0.95	0.05	0.49	0.06
	BV4 1598 1600 (A & B)	16.39	0.89	0.05	0.49	0.06
	BV4 1773 1776 (A & B)	18.15	0.91	0.05	0.48	0.06
	BV4 2096 2098	21.37	0.85	0.05	0.42	0.06
	BV4 2253 2256	22.95	0.85	0.05	0.46	0.06
	BV4 2502 2505	25.44	0.91	0.03	0.46	0.04
	BV4 2830 2833	28.72	1.05	0.03	0.56	0.04
	BV4 2990 2998	30.34	0.84	0.05	0.41	0.04
	BV4 3007 3010	30.49	0.92	0.05	0.46	0.04
Bulk Rock	Dolerite 1	surface	0.23	0.06	0.13	0.05
Buik Rock	Dolerite 2	0.60	0.20	0.06	0.12	0.05
	Dolerite 3	2.20	0.24	0.06	0.12	0.05
Taylor Glacier/Snow	Beacon Valley Fresh Snow (1/5/11)		0.98	0.06	0.51	0.07
,	Taylor Glacier 1		0.86	0.06	0.50	0.05
	Taylor Glacier 2		0.84	0.06	0.40	0.05
	Taylor Glacier Nirvana		1.06	0.06	0.53	0.03

2SD of Mg isotopic values represents two standard deviations of the bracketing standard measurements during a full analytical session.

# 5.2. Controls on permafrost chemistry

# 5.2.1. Evidence of weathering in permafrost sediment

Previous studies have shown the mineral weathering sus ceptibility sequence olivine > pyroxene > amphibole > pla gioclase > K feldspar (Craig and Loughnan, 1964; Colman, 1982; Eggleton et al., 1987; Stefánsson et al., 2001). Therefore, loss of Mg and Ca from pyroxene (and

to a lesser extent, Ca and Na from plagioclase) should be evident in the major element composition of the bulk sedi ment. To look more closely at just dolerite in the per mafrost sediment, we use evidence of a two lithology system from a qualitative XRD analysis showing a system of quartz rich sandstone and dolerite (shown as Mg rich pyroxene and Ca rich plagioclase in an XRD analysis). Using a two end member mixing equation, the percent

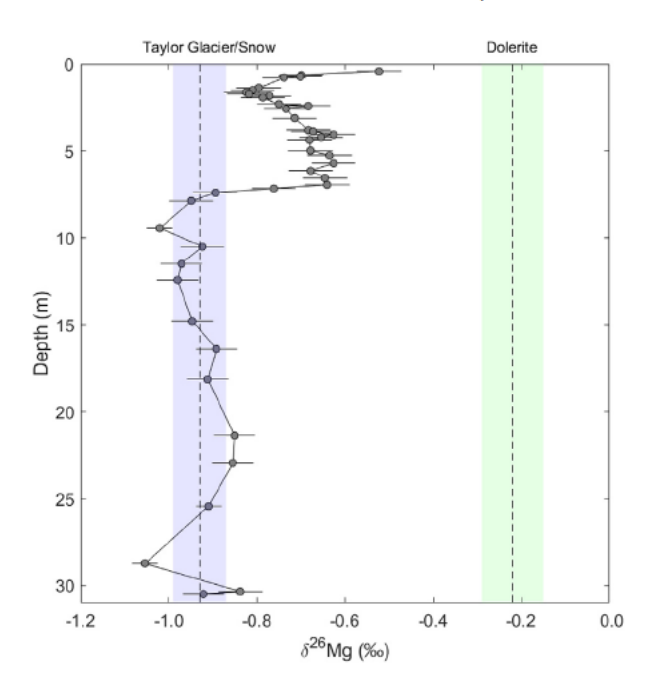


Fig. 4. Mg isotopic analysis of the thawed permafrost ice samples, averaged dolerite rocks, and averaged Taylor Glacier/Beacon snowfall values. The Mg sources in the Antarctica Dry Valleys are shown in the shaded regions. Taylor Glacier/Beacon snowfall (blue) has an Mg isotopic composition of  $0.93\pm0.06\%$  and dolerite (green) has an average value of  $0.22\pm0.07\%$ . Thawed permafrost ice values are plotted in a solid black line. From 0 7 m, the Mg isotopic composition is intermediate between Taylor Glacier/Beacon snowfall and dolerite, and from 7 30 m, the isotopic composition is near or within the range of Taylor Glacier/Beacon snowfall. (For interpretation of the references to colour in this figure legend, the reader is referred to the web version of this article.)

dolerite and sandstone in each sample can be calculated using an immobile element, such as Al<sub>2</sub>O<sub>3</sub> (Nesbitt and Wilson, 1992):

$$Al_2O_{3sandstone} * (X) + Al_2O_{3dolerite} * (1 X)$$

$$= Al_2O_{3sodiment}$$
(1)

where x represents the fraction of sandstone in each sample. The percent of dolerite in each sample can then be used to adjust the major element composition to account for only dolerite sediment in the samples (Fig. 5) to compare to unweathered dolerite values. MgO and CaO show a similar trend for the major element composition. The top four sam ples start off similar to the composition of unweathered dolerite and decrease in concentration moving down to 7.0 m. Below 7.0 m, they are constant and lower than the bulk dolerite composition. K<sub>2</sub>O and Na<sub>2</sub>O both remain constant throughout the core. Na<sub>2</sub>O in each sample has a similar composition to the unweathered dolerite, while K<sub>2</sub>O is higher, suggesting K<sub>2</sub>O may be coming from another source. While there is no granitic bedrock source in Beacon Valley, alkali feldspar rich granite erratics have been found on the Beacon Valley surface and may be an additional source of K2O in the sediment (Dickinson et al., 2017). Muscovite identified in XRD analysis supports

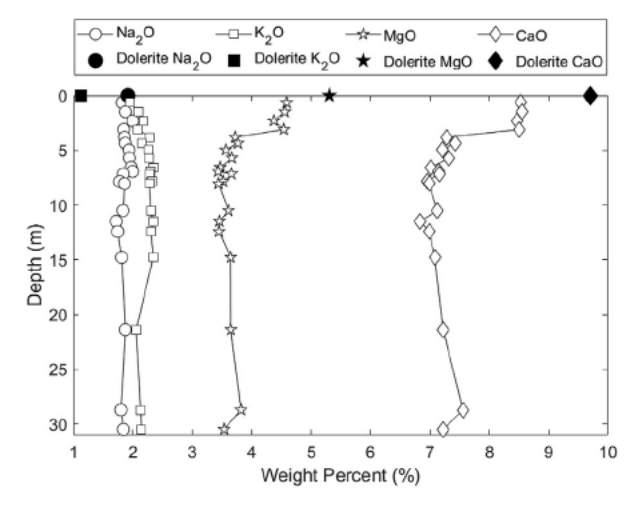


Fig. 5. Major element composition of the  $< 2 \, \text{mm}$  size fraction of CaO,  $K_2O$ , MgO, and  $Na_2O$  (in wt%) normalized to the amount of dolerite in each sample, and unweathered dolerite. CaO and MgO both decrease with depth, while  $K_2O$  and  $Na_2O$  remain constant.

this hypothesis. However, based on the low percentage of muscovite in samples (muscovite <2%) and comparable low MgO concentration in granite erratics compared to dolerite (MgO\_{granite}=0.39 wt%, MgO\_{dolerite}=4.66 wt%), the granite erratics would not have much influence on the MgO composition of the sediment.

Overall, major element composition of the permafrost sediment alone does not show clear evidence for chemical weathering. However, when the major element composition of permafrost sediment is compared to the  $\delta^{26}$ Mg of the thawed permafrost ice, a few trends become apparent (Fig. 6). There is a clear negative correlation between the MgO content of the permafrost sediment and  $\delta^{26}$ Mg values of thawed permafrost ice in the upper 7.0 m ( $R^2 = 0.63$ ). This negative correlation is explained by the loss of Mg from dolerite sediment during dissolution that is docu mented by the decreasing MgO concentration in the sedi ment, and an input of isotopically heavier Mg into the brine released from dolerite weathering, causing the Mg iso topic composition of thawed permafrost ice to become heavier. This trend suggests that the Mg isotopic composi tion of the thawed permafrost ice is controlled by mixing between the two Mg reservoirs rather than fractionation during dissolution. The MgO and  $\delta^{26}$ Mg in the lower 7 30 m do not show a clear correlation ( $R^2 = 0.03$ ), and MgO remains constant.

# 5.2.2. Evidence of chemical weathering in thawed permafrost ice

Chemical weathering is most apparent in pH and Mg isotopic composition of the thawed permafrost ice. Chemical weathering of silicate minerals consumes protons during the dissolution of plagioclase and pyroxene which leads to an increase in pH values. pH values in the core have higher values in the upper 0.40 7.0 m (average = 7.29), lower values in the middle 7.0 18.0 m (average = 7.01), and higher values at 18.0 30.0 m (average = 7.30) (Fig. 2c). While an

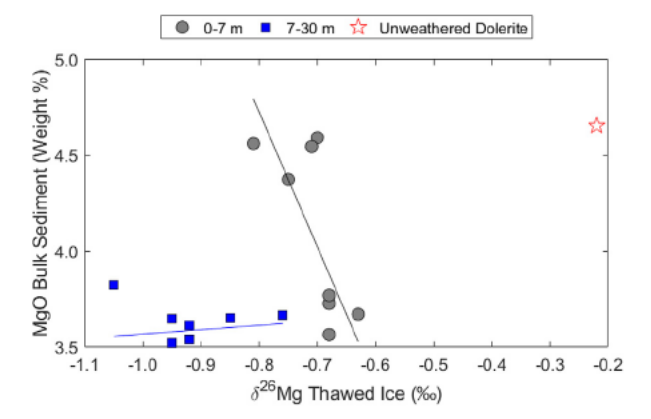
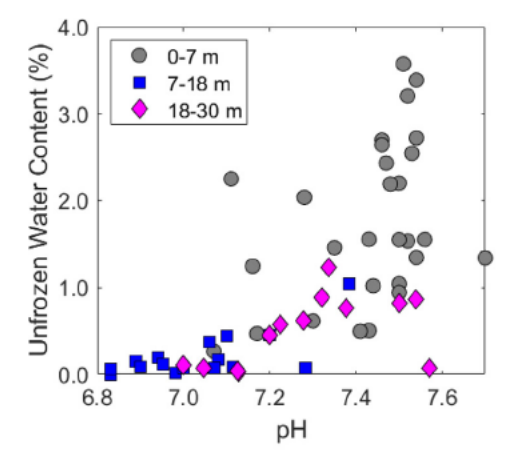


Fig. 6. MgO of bulk sediment corrected for % dolerite (wt%) vs  $\delta^{26}$ Mg (‰) of thawed ice for the upper 0.0 7.0 m, lower 7.0 30.0 m of the core, and unweathered dolerite. The upper 7 m shows a negative correlation where the  $\delta^{26}$ Mg in the thawed ice becomes enriched in the heavy isotope as the MgO content decreases in the bulk sediment. The lower 7 30 m do not show any obvious correlation.

increase in pH with chemical weathering is a known phe nomenon (van Breemen et al., 1983), there are few natural examples of this processes due to leaching of weathering products by percolating water. However, it is apparent in the Beacon Valley core that the weathering products are retained in the ice rich permafrost which leads to the trend observed in the thawed permafrost ice fraction of the sedi ment profile. The pH data are consistent with the weather ing trends revealed in the Mg isotopic composition. Magnesium is released as a weathering product during the hydrolysis of pyroxene. Because the weathering products remain in the ice and the two Beacon Valley Mg reservoirs have such distinct isotopic signatures, sections of the core that experience more chemical weathering have values intermediate between the two end members. This is seen in the upper 0.4 7.0 m, and to a lesser degree in the lower 18.0 30.0 m.



# 5.2.3. Influence of unfrozen water

The main control over chemical weathering is the amount of unfrozen water in the sediment profile, which is modeled as a function of ionic composition of the thawed permafrost ice and temperature. When compared with unfrozen water content, pH and Mg isotopic composition show a similar parabolic curve with a rapid increase in pH and Mg isotopic composition as unfrozen water reaches 1.5% of ice content, and a near constant value when water content is above 1.5% of ice content (Fig. 7). Comparing this trend with sample depth indicates an increase in pH and Mg isotopic ratios in the 0.4 7.0 m and 18.0 30.0 m range. One hypothesis for the parabolic nature of these trends is that as fresh mineral surfaces are initially weath ered, there is a rapid initial consumption of H<sup>+</sup> and release of Mg, followed by a retardation of these processes as the amount of fresh mineral surfaces is reduced (Gérard et al., 2003; White, 2003).

# 5.2.4. Correcting for Mg inputs from marine aerosols in thawed permafrost ice

By correcting for Mg inputs from marine aerosols, we can more closely examine the degree of dissolution and whether any reactions (i.e. secondary mineral precipitation or cation exchange) have changed the ionic or isotopic com position of the thawed permafrost ice samples. This can be done independently using either the Mg concentration or the Mg isotopic composition of the core samples. The Mg concentration in the thawed permafrost ice is corrected for the marine Mg input using a Cl<sup>-</sup> correction as a conser vative ion tracer of marine input (White et al., 2009; Tipper et al., 2010). Because Cl<sup>-</sup> is sourced only from marine aero sols and not chemical weathering (Bao et al., 2008), the Cl<sup>-</sup> correction factor will return the Mg concentration in each sample that is derived only from chemical weathering:

$$Mg_{Cl}^* = Mg_{sample} \quad \left(\frac{Mg}{Cl}\right)_{TG} xCl_{sample}^-$$
 (2)

where  $Mg_{Cl}^*$  is the Mg concentration corrected for marine aerosols, Mg<sub>sample</sub> is the measured Mg concentration of

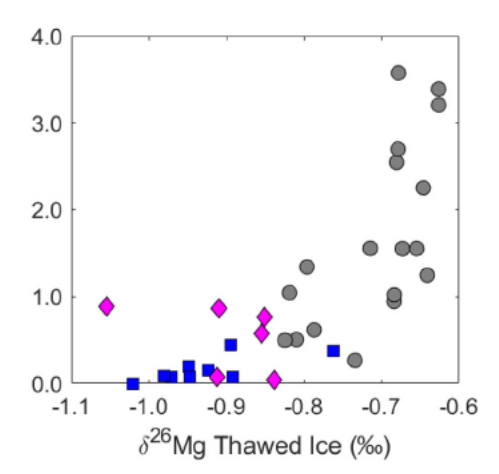


Fig. 7. Modeled unfrozen water content (%) vs pH and  $\delta^{26}$ Mg of the thawed core samples divided into three sections: (1) 0.7 m (black dots), (2) 7.18 m (blue squares), and 18.30 m, (pink diamonds). Each section shows higher pH and  $\delta^{26}$ Mg in regions with higher modeled unfrozen water content. (For interpretation of the references to colour in this figure legend, the reader is referred to the web version of this article.)

each sample (ppm),  $(\frac{Mg}{Cl})_{TG}$  is the ratio of Taylor Glacier/Beacon Snowfall values which represents marine aerosols, and  $Cl_{sample}^-$  is the measured Cl<sup>-</sup> concentration from each sample (ppm). The second constraint that can be used to correct for marine aerosol values is the Mg isotopic composition of the samples (Tipper et al., 2010):

$$Mg_{\delta^{26}Mg}^* = Mg_{sample} \left( \frac{\delta^{26}Mg_{sample} \quad \delta^{26}Mg_{TG}}{\delta^{26}Mg_{dolerite} \quad \delta^{26}Mg_{sample}} \right)$$
(3)

where  $Mg_{\delta^2 \delta_{Mg}}^*$  is the Mg concentration based on isotopic composition,  $\delta^{26} M g_{sample}$  is the isotopic composition of the samples,  $\delta^{26} Mg_{TG}$  is the isotopic composition of Taylor Glacier/Beacon Snowfall, and  $\delta^{26} Mg_{dolerite}$  is the isotopic composition of dolerite. These two calculations indepen dently provide the Mg concentration in the permafrost pro file sourced only from chemical weathering of dolerite. Both cases assume that Mg is only sourced from the two end members, Mg is a conservative element, and that Mg does not participate in any other reactions in the permafrost pro file. Furthermore, the MDV are devoid of vegetation, so vegetation that influences Mg or Cl values are not an issue in these samples. If these assumptions are correct, these two values should be equal and fall along a 1:1 slope (Fig. 8). The calculated values fall nearly along the 1:1 line, with most values in the upper 7.0 m of the core falling slightly above and a few below the 1:1 line. Many of the values below 7.0 m returned negative values (and are not plotted), suggesting loss of Mg to secondary minerals (clays or sec ondary salts) (Tipper et al., 2010). Similarly, the effect of losing Mg from the system on samples that did not return negative values would result in values plotting above the 1:1 line, where  $Mg_{Cl}^*$  would decrease more rapidly than  $Mg_{\delta^{26}Mg}^{*}$  (Tipper et al., 2010).

# 5.2.5. Influence of secondary minerals

These results suggest that secondary Mg clays or salts present in the sediment core may have an influence on the Mg isotopic composition of the thawed permafrost ice sam ples. XRD analysis shows the presence of kaolinite and saponite in the sediment profile, with saponite as the dom inant alteration phase. Saponite is a trioctahedral smectite formed from weathering of mafic rocks with high amounts of structural Mg (as opposed to Mg in interlayer and exchangeable sites) (Borchardt, 1989). Structural Mg that is incorporated into clay mineral octahedral lattice sites pre fer the heavy isotope (Wimpenny et al., 2014), which can lead to the thawed permafrost having a lighter isotopic composition. Secondary salt precipitation may influence the Mg isotopic composition in a similar way. XRD analy sis also reveals small amounts of gypsum (CaSO<sub>4</sub> · 2H<sub>2</sub>O) in two core samples. Coprecipitation of Mg with gypsum has been shown to occur in laboratory experiments, but the amount that coprecipitates with gypsum is small compared to the amount of Mg in solution due to the small partition coefficient between  $0.1 \times 10^{-5}$  and  $4.3 \times 10^{-5}$  (Kushnir, 1980). Another possibility is the formation of epsomite (MgSO<sub>4</sub> · 7H<sub>2</sub>O) and meridianiite (MgSO<sub>4</sub> · 11H<sub>2</sub>O) that may form in trace amounts in MDV sediment. While nei ther mineral is detected by XRD in the Beacon Core sam

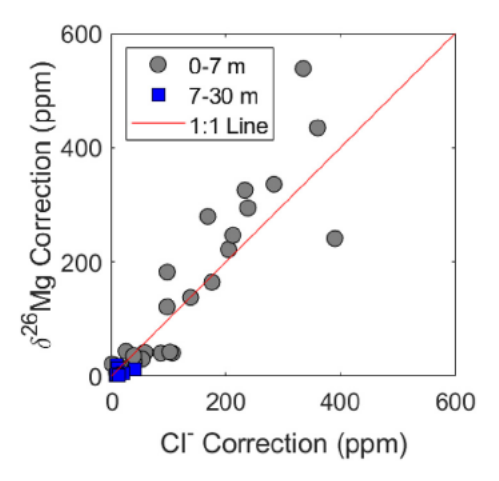


Fig. 8.  $\delta^{26}$ Mg correction vs Cl correction for Mg isotopic and ionic values of the thawed ice. These corrections represent the Mg concentrations derived from chemical weathering and should fall along a 1:1 line if no other processes influence Mg or Cl values.

ples, their presence in trace amounts may affect the Mg isotopes in the thawed permafrost ice significantly given their high Mg concentrations. When either epsomite or meridianiite form, heavy isotopes are preferentially removed from solution and incorporated into the mineral structure of that secondary salt (Li et al., 2011; Schauble, 2011). The average experimental fractionation factor between epsomite and MgSO<sub>4</sub> solution is 0.6% (Li et al., 2011), and the theoretical fractionation factor between meridianiite and MgSO<sub>4</sub> solution is between 0.3 and 2.2% (Li et al., 2011; Schauble, 2011). Both fractionation factors are temperature dependent and have not been calibrated explicitly at subfreezing temperatures. Formation of sec ondary clays and salts along the depth of the core would make the Mg composition of the thawed permafrost ice dependent not just on the two end members, but also on the magnitude of fractionation that occurs during mineral formation. These processes may also explain the two lighter than Taylor Glacier Mg isotopic values in the lower 7.0 30.0 m of the core. While further work is needed to explore the role of secondary minerals and their influence on the Mg isotopic composition at subfreezing tempera tures, the tendency of secondary Mg salts precipitating can be modeled using the ionic composition and tempera ture of the permafrost.

### 5.2.6. Ionic ratios and secondary salts

Secondary salt precipitation can be identified in two ways: (1) using ionic ratios to determine the source of salts to Beacon Valley and trace weathering reactions down the sediment profile; and (2) using PHREEQC modeling to determine the saturation index (where saturation index > 0 predicts the salt will precipitate) of each sample based on the soluble salt concentration and temperature. When eval uating ionic ratios, Cl<sup>-</sup> can be a useful provenance indica tor because it is a most conservative anion and is sourced only from atmospheric inputs (Bao et al., 2008). For most ionic ratios in the core, there is a shift at 7.0 m, suggesting a possible change in source or salt precipitation (Fig. 9).

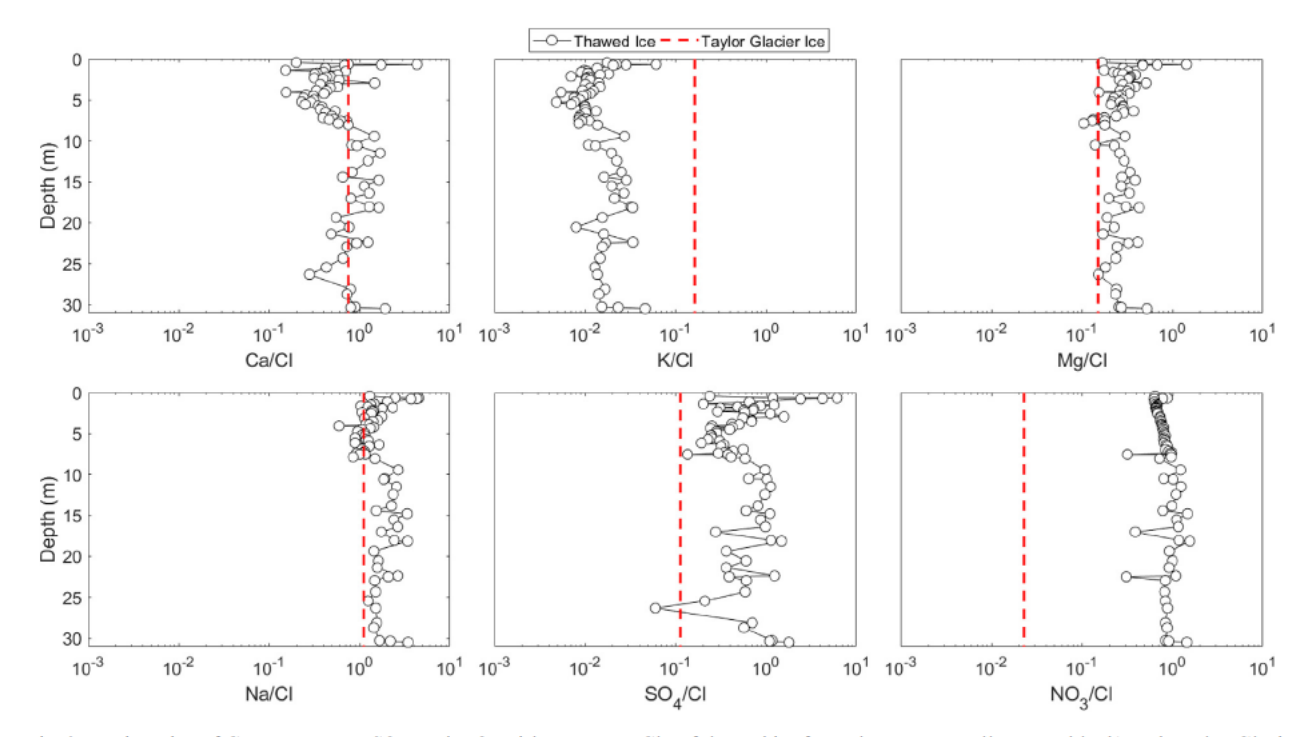


Fig. 9. Ionic ratios of Ca, K, Mg, Na, SO<sub>4</sub>, and NO<sub>3</sub> with respect to Cl of thawed ice from the Beacon Valley core (black) and Taylor Glacier ice (dashed line).

The Ca/Cl ratio and the Na/Cl ratio follow a similar trend, where both are lower in the upper 7.0 m and higher in the lower 7.0 30.0 m. This trend is also seen in the SO<sub>4</sub>/Cl ratio, suggesting formation of calcium and sodium sulfates. When modeled in PHREEQC, precipitation of gypsum (CaSO<sub>4</sub>·2H<sub>2</sub>O) and mirabilite (Na<sub>2</sub>SO<sub>4</sub>·10H<sub>2</sub>O) occurs throughout the core, with the highest saturation index occurring in the upper 7.0 m (Fig. 10). The Mg/Cl ratios

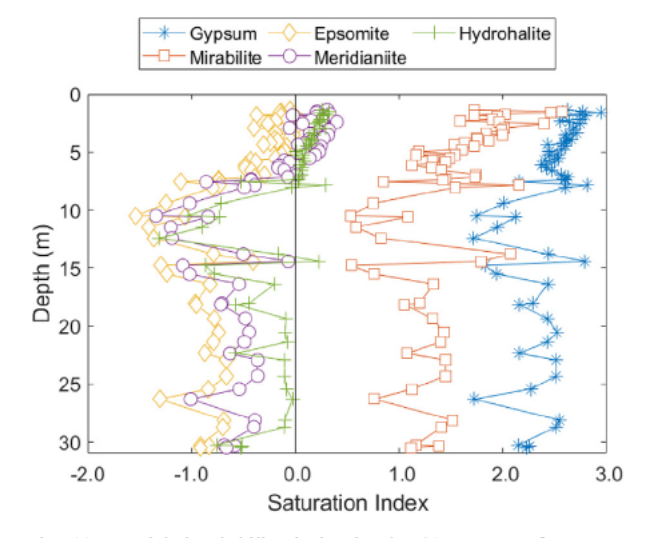


Fig. 10. Modeled solubility index in the 30 m core of gypsum, mirabilite, epsomite, meridianiite, and hydrohalite based on temperature and soluble salt concentration. The models indicate that all five salts can precipitate in the core.

follow an opposite trend as Ca/Cl and Na/Cl. The Mg/Cl ratio in the upper section of the core is greater than that in the lower section of the core. One possible explanation for the shift in the Mg/Cl ratio is a greater amount of Mg is released from dissolution and a smaller amount of Mg is consumed by precipitation reactions compared to Ca or Na. Evidence from Mg isotopes and pH supports a greater amount of dissolution in the upper 7.0 m. Furthermore, Mg salts are more soluble than Ca and Na salts (Kushnir, 1980), and there will be a smaller amount of sulfate avail able to precipitate with Mg in the brine after it is consumed by gypsum and mirabilite precipitation. Nonetheless, chem ical models show small amounts of magnesium sulfates pre cipitating in the form of meridianiite (MgSO<sub>4</sub>·11H<sub>2</sub>O) and epsomite (MgSO<sub>4</sub>·7H<sub>2</sub>O). PHREEQC modeling results of secondary Mg salts precipitating may explain why samples fall above the 1:1 line when correcting Mg ions and Mg iso topes for marine aerosols (Fig. 8). Overall, secondary salts, including gypsum (CaSO<sub>4</sub>·2H<sub>2</sub>O), mirabilite (Na<sub>2</sub>SO<sub>4</sub> ·10H2O), epsomite (MgSO4·7H2O), meridianiite (MgSO4 ·11H<sub>2</sub>O), and hydrohalite (NaCl·2H<sub>2</sub>O) all are modeled to form within the core. The low temperature database for PHREEQC does not contain nitrate and those species were not modeled.

# 5.3. Degree of chemical weathering

The degree of weathering based on the Mg isotopic com position in the thawed ice can be calculated using a mass balance equation of the two end member system:

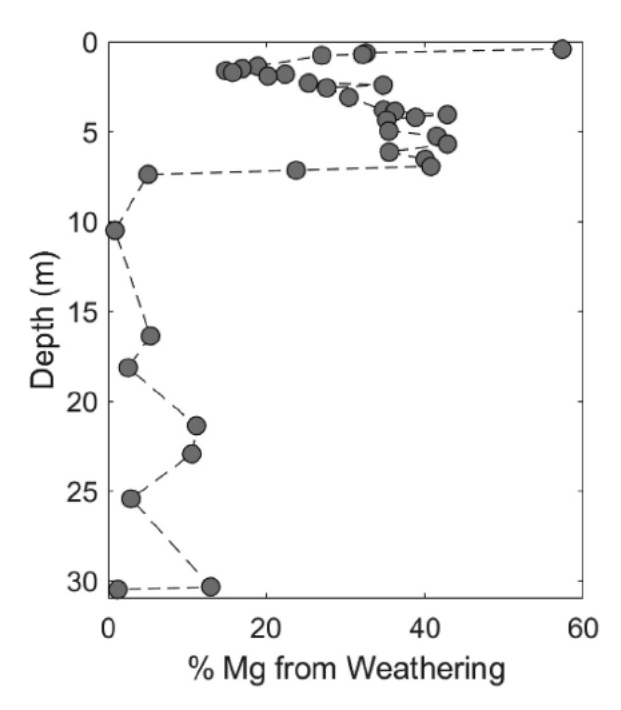


Fig. 11. The percentage of Mg derived from dissolution of dolerite in the Beacon Valley core for a Taylor Glacier end member. More dissolution occurs in the upper section of the core compared to the lower section of the core.

$$\% Weathering = \frac{\delta^{26} Mg_{sample}}{\delta^{26} Mg_{dolerite}} \frac{\delta^{26} Mg_{TG}}{\delta^{26} Mg_{TG}}$$

$$\tag{4}$$

Fig. 11 plotted the calculated degree of weathering of Beacon Valley core using eq (4). Since these values do not consider potential fractionation from secondary mineral formation, they provide a conservative estimate of chemical weathering. In the upper 7.0 m, two distinct trends are seen. The highest degree of weathering occurs from 0.40 to 1.5 m, where up to 60% of Mg sourced from weathering. At 1.6 m, weathering contributes approximately 20% of Mg, and increases to near 42% at 7.0 m. The amount of Mg derived from dolerite weathering increases rapidly from 1.6 m to 4.0 m, and then remains constant at around 40% from 4.0 to 7.0 m. In the lower 7.0 30 m, weathering contributes a range of 0 20% of Mg to the permafrost and increases with depth in the core.

# 5.4. Implications

Chemical weathering of silicate rocks is one of the pri mary sinks of carbon dioxide from the atmosphere over long time scales (Berner, 1992). To understand and quantify chemical weathering on a continental and global scale, weathering must be studied under a variety of climatic con ditions and geologic settings, including cold and dry permafrost dominated regions. These data provide impor tant steps towards understanding and quantifying silicate weathering over time in permafrost dominated regions. Our study of chemical weathering in the ice cemented per mafrost profile demonstrates that even in the cold and dry

environment of the MDV, in situ rock water interactions leads to significant weathering. Since permafrost dominated soils occur in over 20% of the ice free surfaces on Earth, weathering here cannot be discounted.

Furthermore, our results indicate the extent of chemical weathering in cold and dry permafrost environments depends on the ionic content and the temperature. An important finding of our study supports the concept of a "eutectic layer active zone", where unfrozen water (and chemical weathering) is present to the depth at which the maximum temperature exceeds the eutectic point of the dominant salt. In this study, the dominant salt is NaCl with a eutectic temperature of 21 °C, which is the maximum temperature below 7.0 m where there is limited to no chem ical weathering in the sediment core. The findings here have implications for studies of areas such as Don Juan Pond, which is dominated by CaCl<sub>2</sub> salts with a eutectic point of 50.4 °C (Marion, 1997), and the martian environment, where perchlorates lower the eutectic point to as low as 74.6 °C (Marion et al., 2010). Regions with such low eutectic points may experience chemical weathering and see a higher content of unfrozen water extending to deeper depths than previously thought.

#### 6. CONCLUSIONS

This study provides direct evidence of chemical weather ing in ice rich permafrost in the McMurdo Dry Valleys. The continuously frozen permafrost allows weathering products to accumulate in the ice rich sediments, thereby, uniquely documenting in situ chemical weathering in per mafrost over long time scales. The evidence of chemical weathering is recorded in the elemental composition of the permafrost sediment, the Mg isotopic composition, pH, and ionic ratios of the thawed permafrost ice, and is strongly correlated to the percent of unfrozen water con tent. This work provides important conclusions about the history of chemical weathering processes in cold and dry environments:

- (1) Evidence for chemical weathering based on salts, pH, and Mg isotopes shows weathering occurred in the upper 7.0 m of ice cemented permafrost, where up to 60% of Mg is derived from dolerite. In the lower 7.0 30 m, less weathering occurs with an average of 5% of Mg sourced from dolerite weathering.
- (2) The unfrozen water, as modeled using ground tem perature and soluble salt concentration, is the major control on the degree of weathering. The evidence supporting weathering includes a heavier Mg isotopic composition due to dolerite dissolution and higher pH due to proton consumption; both are more pro nounced where there is a higher percentage of unfro zen water. The temperatures at which we see unfrozen water suggests that chemical weathering occurs when ground temperatures exceed the eutectic point of the dominant salt and unfrozen water is pre sent even deep within the permafrost core at subzero temperatures.

(3) Secondary minerals may have a small influence on Mg isotopic composition in Beacon Valley. Fraction ation caused by clay formation and secondary salt precipitation may explain why  $Mg_{Cl}^*$  and  $Mg_{\delta^{26}Mg}^*$  correction values do not fall along a 1:1 line, and the Mg values that are lighter than Taylor Glacier in the lower 7.0 3.0 m. Further work is needed to constrain secondary minerals and the temperature dependence of fractionation factors in permafrost conditions.

# **ACKNOWLEDGEMENTS**

Financial and logistic support is provided by Grant Nos. OPP 1341680 and OPP 0636998 from the National Science Foundation, United States and Grant 80NSSC17K0715 from NASA. Funding was also provided by the GSA Graduate Student Research Grant and the Vance Fellowship in Geology Science. Drilling support and equipment was contracted from Webster Drilling and Exploration Limited, Wellington, New Zealand. Special thanks to the XRD analysis and interpretation provided by Doug Ming and Val erie Tu at the NASA Johnson Space Center. We are also grateful for the the insightful reviews by C. McKay, who suggested using the term "Eutectic layer active zone," W. Dickinson, an anony mous reviewer, and Guest Editor Xiao Ming Liu.

#### REFERENCES

- Alberdi M., Bravo L. A., Gutiérrez A., Gidekel M. and Corcuera L. J. (2002) Ecophysiology of Antarctic vascular plants. *Physiol. Plant.* 115, 479 486.
- Anderson D. M., Gatto L. and Ugolini F. C. (1972) An Antarctic analog of Martian permafrost terrain. Antarct J. Unit States 7, 114-116
- Anderson D. M. and Morgenstern N. (1973) Physics, chemistry, and mechanics of frozen ground: a review. In *Permafrost: The North American Contribution to the Second International Con* ference, National Academy of Sciences, Washington, DC, pp. 257–288.
- Bao H., Barnes J. D., Sharp Z. D. and Marchant D. R. (2008) Two chloride sources in soils of the McMurdo Dry Valleys, Antarctica. *J Geophys. Res.: Atmospheres* 113.
- Bao H., Campbell D. A., Bockheim J. G. and Thiemens M. H. (2000) Origins of sulphate in Antarctic dry valley soils as deduced from anomalous 17O compositions. *Nature* 407, 499 502.
- Berner R. A. (1992) Weathering, plants, and the long term carbon cycle. *Geochim. Cosmochim. Acta* **56**, 3225–3231.
- Bockheim J. G. (1995) Permafrost distribution in the southern circumpolar region and its relation to the environment: a review and recommendations for further research. *Permafrost Peri glac. Process.* **6**, 27–45.
- Bockheim J. G., Kurz M. D., Soule S. A. and Burke A. (2009) Genesis of active sand filled polygons in lower and central Beacon Valley, Antarctica. *Permafrost Periglacial Processes* **20** (3), 295–308.
- Borchardt G. (1989) Smectites. In *Minerals in soil environments*, (mineralsinsoile), pp. 675–727.
- Bromley A. M. (1985) Weather observations Wright Valley, Antarctica. New Zealand Antarctic Research Programme. Vanda Station.
- Campbell I. B. and Claridge G. (1987) Antarctica: Soils, Weather ing Processes and Environment. Elsevier.

- Chinn T. (1990). In *The dry valleys. Antarctica; the Ross Sea region DSIR Information Series*, pp. 137–153.
- Claridge G. and Campbell I. (1977) The salts in Antarctic soils, their distribution and relationship to soil processes. *Soil Sci.* **123**, 377 384.
- Colman S. M. (1982) Chemical Weathering of Basalts and Ande sites; Evidence from Weathering Rinds. USGPO.
- Craig D. and Loughnan F. (1964) Chemical and mineralogical transformations accompanying the weathering of basic volcanic rocks from New South Wales. Soil Res. 2, 218 234.
- De Villiers S., Dickson J. and Ellam R. (2005) The composition of the continental river weathering flux deduced from seawater Mg isotopes. *Chem. Geol.* **216**, 133–142.
- Diaz M. A., Adams B. J., Welch K. A., Welch S. A., Opiyo S. O., Khan A. L. and Lyons W. B. (2018) Aeolian material transport and its role in landscape connectivity in the Mcmurdo Dry Valleys, Antarctica. J. Geophys. Res. Earth Surf. 123(12), 3323 3337.
- Dickinson W. W. and Grapes R. H. (1997) Authigenic chabazite and implications for weathering in Sirius group diamictite, Table Mountain, Dry Valleys, Antarctica. J. Sediment. Res. 67, 815–820.
- Dickinson W. W. and Rosen M. R. (2003) Antarctic permafrost: An analogue for water and diagenetic minerals on Mars. Geology 31, 199 202.
- Dickinson W. W., Williams G., Hill M., Cox S. C. and Baker J. A. (2017) Granite erratics in Beacon Valley, Antarctica. *Antarct. Sci.* 29, 343–355.
- Doran P. T., McKay C. P., Clow G. D., Dana G. L., Fountain A. G., Nylen T. and Lyons W. B. (2002) Valley floor climate observations from the McMurdo Dry Valleys, Antarctica, 1986 2000. J. Geophys. Res.: Atmos. 107.
- Dowling C. B., Lyons W. and Welch K. A. (2013) Strontium isotopic signatures of streams from Taylor Valley, Antarctica, Revisited: the role of carbonate mineral dissolution. *Aquat. Geochem.* 19, 231–240.
- Eggleton R. A., Foudoulis C. and Varkevisser D. (1987) Weather ing of basalt: changes in rock chemistry and mineralogy. *Clays Clay Miner*. 35, 161–169.
- Elliot D., Fleming T., Haban M. and Siders M. (1995) Petrology and mineralogy of the Kirkpatrick basalt and Ferrar dolerite, Mesa range region, North Victoria Land, Antarctica. Contrib. Antarctic Res. IV, 103-141.
- Fountain A. G., Nylen T. H., Monaghan A., Basagic H. J. and Bromwich D. (2010) Snow in the McMurdo Dry Valleys, Antarctica. *Int. J. Climatol.* **30**, 633–642.
- Galy A., Bar Matthews M., Halicz L. and O'Nions R. K. (2002) Mg isotopic composition of carbonate: insight from speleothem formation. *Earth Planet. Sci. Lett.* 201, 105–115.
- Gérard F., Ranger J., Ménétrier C. and Bonnaud P. (2003) Silicate weathering mechanisms determined using soil solutions held at high matric potential. *Chem. Geol.* **202**, 443 460.
- Gibson E. K., Wentworth S. J. and McKay D. S. (1983) Chemical weathering and diagenesis of a cold desert soil from Wright Valley, Antarctica: an analog of Martian weathering processes. J. Geophys. Res.: Solid Earth 88.
- Green W. J., Angle M. P. and Chave K. E. (1988) The geochemistry of Antarctic streams and their role in the evolution of four lakes of the McMurdo Dry Valleys. *Geochim. Cosmochim. Acta* 52, 1265–1274.
- Gunn B. M. (1962) Differentiation in ferrar dolerites, Antarctica. N. Z. J. Geol. Geophys. 5, 820 863.
- Hagedorn B., Sletten R. S., Hallet B., McTigue D. F. and Steig E. J. (2010) Ground ice recharge via brine transport in frozen soils of Victoria Valley, Antarctica: insights from modeling δ 18 O and δD profiles. Geochim. Cosmochim. Acta 74, 435–448.

- Hall B. L. and Denton G. H. (2002) Holocene history of the Wilson Piedmont Glacier along the southern Scott Coast, Antarctica. *The Holocene* 12, 619–627.
- Heindel R. C., Lyons W. B., Welch S. A., Spickard A. M. and Virginia R. A. (2018) Biogeochemical weathering of soil apatite grains in the McMurdo Dry Valleys, Antarctica. *Geoderma* 320, 136–145.
- Heldmann J., Pollard W., McKay C., Marinova M., Davila A., Williams K., Lacelle D. and Andersen D. (2013) The high elevation Dry Valleys in Antarctica as analog sites for subsurface ice on Mars. *Planet. Space Sci.* 85, 53–58.
- Hu Y., Harrington M. D., Sun Y., Yang Z., Konter J. and Teng F. Z. (2016) Magnesium isotopic homogeneity of San Carlos olivine: a potential standard for Mg isotopic analysis by multi collector inductively coupled plasma mass spectrometry. *Rapid Commun. Mass Spectrom.* 30, 2123–2132.
- Huang K. J., Teng F. Z., Wei G. J., Ma J. L. and Bao Z. Y. (2012)
   Adsorption and desorption controlled magnesium isotope fractionation during extreme weathering of basalt in Hainan Island, China. *Earth Planet. Sci. Lett.* 359 360, 73 83.
- Jones L. M. and Faure G. (1978) A study of strontium isotopes in lakes and surficial deposits of the ice free valleys, southern Victoria Land, Antarctica. *Chem. Geol.* 22, 107–120.
- Keys J. H. and Williams K. (1981) Origin of crystalline, cold desert salts in the McMurdo region, Antarctica. *Geochim. Cosmochim.* Acta 45, 2299–2309.
- Kushnir J. (1980) The coprecipitation of strontium, magnesium, sodium, potassium and chloride ions with gypsum. An exper imental study. Geochim. Cosmochim. Acta 44, 1471 1482.
- Leslie D., Lyons W. B., Warner N., Vengosh A., Olesik J., Welch K. and Deuerling K. (2014) Boron isotopic geochemistry of the McMurdo Dry Valley lakes, Antarctica. Chem. Geol. 386, 152–164.
- Li W., Beard B. L. and Johnson C. M. (2011) Exchange and fractionation of Mg isotopes between epsomite and saturated MgSO 4 solution. *Geochim. Cosmochim. Acta* 75, 1814–1828.
- Li W. Y., Teng F. Z., Ke S., Rudnick R. L., Gao S., Wu F. Y. and Chappell B. (2010) Heterogeneous magnesium isotopic composition of the upper continental crust. *Geochim. Cosmochim.* Acta 74, 6867–6884.
- Ling M. X., Sedaghatpour F., Teng F. Z., Hays P. D., Strauss J. and Sun W. (2011) Homogeneous magnesium isotopic composition of seawater: an excellent geostandard for Mg isotope analysis. *Rapid Commun. Mass Spectrom.* 25, 2828–2836.
- Linkletter G., Bockheim J. and Ugolini F. (1973) Soils and glacial deposits in the Beacon Valley, southern Victoria Land, Antarctica. N. Z. J. Geol. Geophys. 16, 90 108.
- Liu L., Sletten R. S., Hagedorn B., Hallet B., McKay C. P. and Stone J. O. (2015) An enhanced model of the contemporary and long term (200 ka) sublimation of the massive subsurface ice in Beacon Valley, Antarctica. *J. Geophys. Res. Earth Surf.* 120, 1596 1610.
- Liu X. M., Teng F. Z., Rudnick R. L., McDonough W. F. and Cummings M. L. (2014) Massive magnesium depletion and isotope fractionation in weathered basalts. *Geochim. Cos mochim. Acta* 135, 336–349.
- Lyons W. B., Bullen T. D. and Welch K. A. (2017) Ca isotopic geochemistry of an Antarctic aquatic system. *Geophys. Res. Lett.* **44**, 882–891.
- Lyons W. B. and Mayewski P. A. (1993) The geochemical evolution of terrestrial waters in the Antarctic: the role of rock water interactions. *Phys. Biogeochem. Processes Antarctic Lakes* **59**, 135–143.
- Low P. F., Anderson D. M. and Hoekstra P. (1968) Some thermodynamic relationships for soils at or below the freezing point: 1. Freezing point depression and heat capacity. *Water Resour. Res.* 4, 379–394.

- Ma L., Teng F. Z., Jin L., Ke S., Yang W., Gu H. O. and Brantley S. L. (2015) Magnesium isotope fractionation during shale weathering in the Shale Hills Critical Zone Observatory: accumulation of light Mg isotopes in soils by clay mineral transformation. *Chem. Geol.* 397, 37–50.
- Marion G. M. (1997) A theoretical evaluation of mineral stability in Don Juan Pond, wright valley, victoria land. *Antarct. Sci.* 9 (1), 92–99.
- Marion G. M., Catling D. C., Zahnle K. J. and Claire M. W. (2010) Modeling aqueous perchlorate chemistries with applica tions to Mars. *Icarus* 207(2), 675–685.
- Marion G. M. and Grant S. A. (1994) FREZCHEM: A CHEMICAL Thermodynamic Model for Aqueous Solutions at Subzero Temperatures. DTIC Document.
- Marra K. R., Madden M. E. E., Soreghan G. S. and Hall B. L. (2017) Chemical weathering trends in fine grained ephemeral stream sediments of the McMurdo Dry Valleys, Antarctica. *Geomorphology* 281, 13–30.
- Maurice P. A., McKnight D. M., Leff L., Fulghum J. E. and Gooseff M. (2002) Direct observations of aluminosilicate weathering in the hyporheic zone of an Antarctic Dry Valley stream. Geochim. Cosmochim. Acta 66, 1335–1347.
- McElroy C. and Rose G. (1987) Geology of the Beacon Heights area, southern Victoria Land, Antarctica. *New Zealand Geol. Survey Miscell. Ser. Map* 15.
- Michalski G., Bockheim J., Kendall C. and Thiemens M. (2005) Isotopic composition of Antarctic Dry Valley nitrate: implications for NOy sources and cycling in Antarctica. *Geophys. Res. Lett.* 32.
- Murrmann R. P. (1973) Ionic mobility in permafrost. In Proceed ings of the Second International Conference on Permafrost, Yakutsk, pp. 352–359.
- Nesbitt H. and Wilson R. (1992) Recent chemical weathering of basalts. *Am. J. Sci.* **292**, 740 777.
- Nezat C. A., Lyons W. B. and Welch K. A. (2001) Chemical weathering in streams of a polar desert (Taylor Valley, Antarctica). Geol. Soc. Am. Bull. 113, 1401 1408.
- Opfergelt S., Burton K., Georg R., West A., Guicharnaud R., Sigfusson B., Siebert C., Gislason S. and Halliday A. (2014)
  Magnesium retention on the soil exchange complex controlling
  Mg isotope variations in soils, soil solutions and vegetation in volcanic soils, Iceland. Geochim. Cosmochim. Acta 125, 110
  130
- Opfergelt S., Georg R., Delvaux B., Cabidoche Y. M., Burton K. and Halliday A. (2012) Mechanisms of magnesium isotope fractionation in volcanic soil weathering sequences, Guade loupe. *Earth Planet. Sci. Lett.* 341, 176–185.
- Pettit E. C., Whorton E. N., Waddington E. D. and Sletten R. S. (2014) Influence of debris rich basal ice on flow of a polar glacier. J. Glaciol. 60, 989 1006.
- Pogge von Strandmann P. A. E., Burton K. W., James R. H., van Calsteren P., Gislason S. R. and Sigfússon B. (2008) The influence of weathering processes on riverine magnesium isotopes in a basaltic terrain. *Earth Planet. Sci. Lett.* **276**, 187 197.
- Pogge von Strandmann P. A. E., Opfergelt S., Lai Y. J., Sigfússon B., Gislason S. R. and Burton K. W. (2012) Lithium, magnesium and silicon isotope behaviour accompanying weathering in a basaltic soil and pore water profile in Iceland. *Earth Planet. Sci. Lett.* 339, 11 23.
- Schaefer C. E. G., Michel R. F., Delpupo C., Senra E. O., Bremer U. F. and Bockheim J. G. (2017) Active layer thermal monitoring of a Dry Valley of the Ellsworth Mountains, Continental Antarctica. *Catena* 149, 603–615.
- Schauble E. A. (2011) First principles estimates of equilibrium magnesium isotope fractionation in silicate, oxide, carbonate

- and hexaaquamagnesium (2+) crystals. *Geochim. Cosmochim.* Acta 75, 844-869.
- Sletten R., Hallet B. and Fletcher R. (2003) Resurfacing time of terrestrial surfaces by the formation and maturation of polyg onal patterned ground. J. Geophys. Res. Planets 108.
- Stefánsson A., Gı'slason S. R. and Arnórsson S. (2001) Dissolution of primary minerals in natural waters: II. Mineral saturation state. Chem. Geol. 172, 251–276.
- Tamppari L., Anderson R., Archer P., Douglas S., Kounaves S., McKay C., Ming D., Moore Q., Quinn J. and Smith P. (2012) Effects of extreme cold and aridity on soils and habitability. McMurdo Dry Valleys as an analogue for the Mars Phoenix landing site. *Antarct. Sci.* 24, 211 228.
- Teng F. Z., Li W. Y., Rudnick R. L. and Gardner L. R. (2010) Contrasting lithium and magnesium isotope fractionation during continental weathering. *Earth Planet. Sci. Lett.* 300, 63 71.
- Teng F. Z., Wadhwa M. and Helz R. T. (2007) Investigation of magnesium isotope fractionation during basalt differentiation: implications for a chondritic composition of the terrestrial mantle. *Earth Planet. Sci. Lett.* 261, 84 92.
- Teng F. Z., Li W. Y., Ke S., Yang W., Liu S. A., Sedaghatpour F., Wang S. J., Huang K. J., Hu Y. and Ling M. X. (2015) Magnesium isotopic compositions of international geological reference materials. *Geostand. Geoanal. Res.* 39, 329–339.
- Teng F. Z. and Yang W. (2014) Comparison of factors affecting the accuracy of high precision magnesium isotope analysis by multi collector inductively coupled plasma mass spectrometry. *Rapid Commun. Mass Spectrom.* 28, 19–24.
- Teng F. Z. (2017) Magnesium isotope geochemistry. Rev. in Mineral. Geochem. 82, 219 287.
- Tice A. R., Yuanlin Z. and Oliphant J. (1985) The effects of soluble salts on the unfrozen water contents of the Lanzhou, PRC, silt. *J. Glaciol. Geocryol.* 2.
- Tipper E. T., Calmels D., Gaillardet J., Louvat P., Capmas F. and Dubacq B. (2012a) Positive correlation between Li and Mg isotope ratios in the river waters of the Mackenzie Basin challenges the interpretation of apparent isotopic fractionation during weathering. *Earth Planet. Sci. Lett.* 333, 35 45.

- Tipper E. T., Gaillardet J., Louvat P., Capmas F. and White A. F. (2010) Mg isotope constraints on soil pore fluid chemistry: evidence from Santa Cruz, California. *Geochim. Cosmochim.* Acta 74, 3883–3896.
- Tipper E. T., Lemarchand E., Hindshaw R. S., Reynolds B. C. and Bourdon B. (2012b) Seasonal sensitivity of weathering processes: hints from magnesium isotopes in a glacial stream. *Chem. Geol.* **312**, 80–92.
- van Breemen N., Mulder J. and Driscoll C. (1983) Acidification and alkalinization of soils. *Plant Soil* **75**, 283–308.
- Wentworth S. J., Gibson E. K., Velbel M. A. and McKay D. S. (2005) Antarctic Dry Valleys and indigenous weathering in Mars meteorites: implications for water and life on Mars. *Icarus* **174**, 383–395.
- White A. (2003) Natural weathering rates of silicate minerals. *Treatise Geochem.* **5**, 605.
- White A. F., Schulz M. S., Stonestrom D. A., Vivit D. V., Fitzpatrick J., Bullen T. D., Maher K. and Blum A. E. (2009) Chemical weathering of a marine terrace chronosequence, Santa Cruz, California. Part II: Solute profiles, gradients and the comparisons of contemporary and long term weathering rates. Geochim. Cosmochim. Acta 73, 2769 2803.
- Wimpenny J., Colla C. A., Yin Q. Z., Rustad J. R. and Casey W. H. (2014) Investigating the behaviour of Mg isotopes during the formation of clay minerals. *Geochim. Cosmochim. Acta* 128, 178–194.
- Witherow R. A., Lyons W. B. and Henderson G. M. (2010) Lithium isotopic composition of the McMurdo Dry Valleys aquatic systems. Chem. Geol. 275, 139 147.
- Yang W., Teng F. Z. and Zhang H. F. (2009) Chondritic magne sium isotopic composition of the terrestrial mantle: a case study of peridotite xenoliths from the North China craton. *Earth Planet. Sci. Lett.* 288, 475–482.
- Zhang T., Barry R. G., Knowles K., Heginbottom J. and Brown J. (1999) Statistics and characteristics of permafrost and ground ice distribution in the Northern Hemisphere. *Polar Geogr.* 23, 132–154.

Associate editor: Xiao Ming Liu